Supplementary Material: Simulated water table with MODFLOW

We set up a MODFLOW-2005 (Harbaugh, 2005) model to simulate the problem that we used as example in the main article. Figure S1 shows a schematic of the numerical model. Initially we setup a model with a grid spacing equal to 1 m in the vertical and horizontal directions (20 layers and 100 columns). We used the DE4 direct solver as linear solver, however we also used the default PCG solver for preliminary simulation, obtaining similar results. We only considered the heterogeneous case with $K_2 = K_1/100$, since preliminary simulations demonstrated that cases with less difference in the values of K were easier to solve.

This setting was chosen as example because it represents well a real-world problem analyzed by the authors and also because it provides the simplest possible example for a heterogeneous unconfined aquifer that can be simulated with MODFLOW. It turned out to be difficult to obtain a reliable numerical solution for this setting because of convergence problems. We could obtain only approximated solutions that did not satisfy the default convergence criteria used in MODFLOW, which are shown in Figures S2 to S6. The convergence problems were due to the rewetting of cells that dried up and were converted to inactive cells during the iterative solution. The numerical solution proved to be also significantly sensitive to other settings such as grid size, initial hydraulic head and number of iterations for the non-linear solver.

The solutions computed with the original 1 m grid were too coarse (Figures S2 and S3), hence we refined the grid to obtain cells with 10 cm spacing in the vertical and horizontal directions (Figures S4-S6), i.e. the refined grid has 200 layers and 1000 columns. The best simulated solution is shown in Figure S4. In contrast to the assumption of low vertical gradients considered to derive the analytical solution, the numerical solution demonstrates that the mounding produced by recharge results in a water table that has steep slope within material 2, hence important vertical gradients within that material.

Figure S7 shows a comparison between the analytical solution used in the article and numerical solutions computed with MODFLOW for cells along a row that coincides with the elevation of the left boundary condition (z = 10 m). It is not possible to compare directly both numerical solutions to the analytical one, because of the assumptions that were considered to derive the later. Moreover, the analytical solution represents the elevation of the water table, while values that correspond to the numerical solutions are the piezometric head computed along a row of the model, i.e. at a constant elevation. However, the analytical and numerical solutions are close to each other and consider a mounding of similar magnitude within material 2 (lower K). Refining the grid results in an increase in the maximum simulated piezometric head (at the flow divide within material 2) of 33 cm compared to the coarser grid. The difference in the maximum head between the analytical and the refined numerical solution is 57 cm. On the other hand, all three solutions are almost identical within material 1. This comparison demonstrates that the analytical solution is a reasonable representation of the expected water table. It also demonstrates the magnitude of potential differences between numerical solutions, which should be considered when comparing simulated values against observations.

The convergence problems encountered while trying to set up the simulations and the differences between the numerical solutions were deterrent for the use of a purely numerical approach based on the use of MODFLOW and PEST (Doherty & Hunt, 2010; Doherty, 2015) for the analysis of the solution of the inverse problem. Moreover, the solution for the value of the piezometric head as function of the parameters of the problem (values of hydraulic conductivity) is highly non-linear as shown in Figure S8, which was prepared based on the analytical model. Hence, it is likely that any technique based on the linearization of the problem will have some difficulties to converge to the true solution.

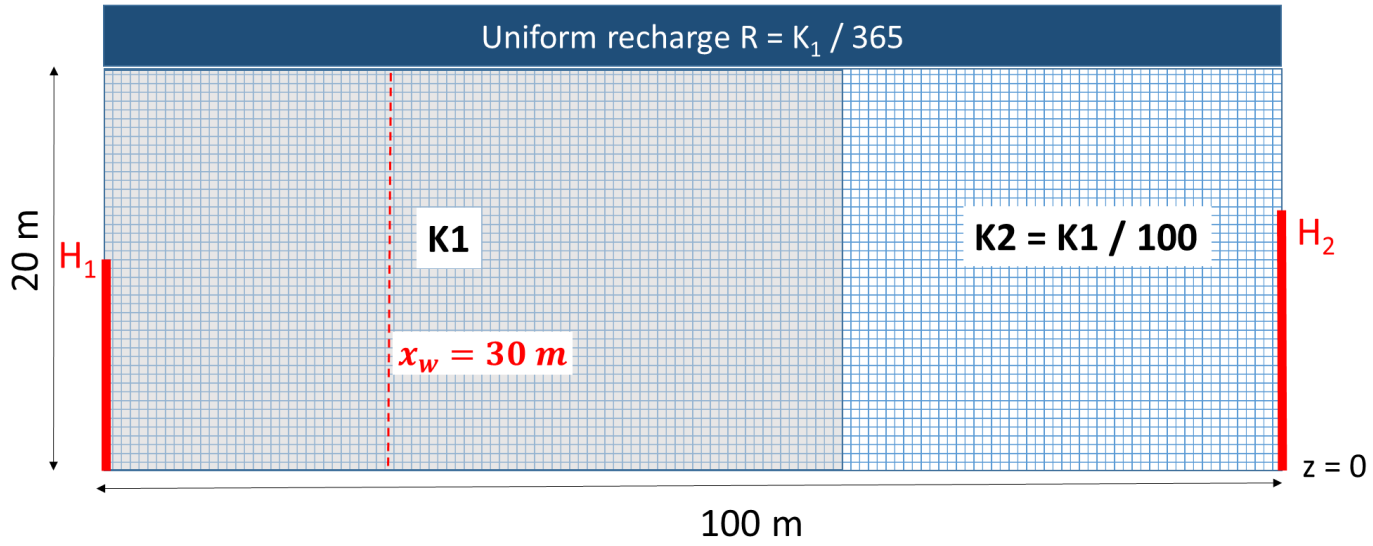

Figure S1: Schematic of set up for numerical simulation.

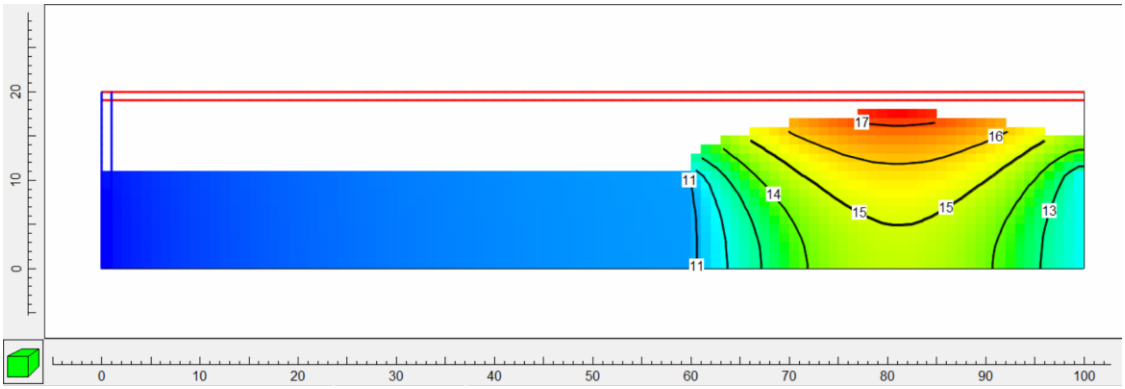

Figure S2: Simulated piezometric head in a grid spacing equal to 1 m considering initial head equal to 22 m. Colors represent values of piezometric head, black lines show iso-contours and axes indicate distance in the horizontal and vertical directions in meters.

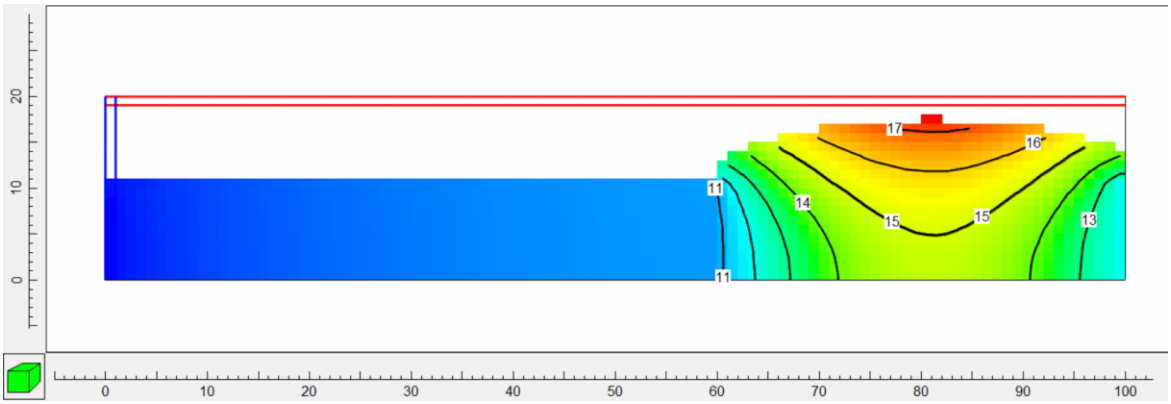

Figure S3: Simulated piezometric head in a grid spacing equal to 1 m considering initial head equal to 12.5 m. Colors represent values of piezometric head, black lines show iso-contours and axes indicate distance in the horizontal and vertical directions in meters.

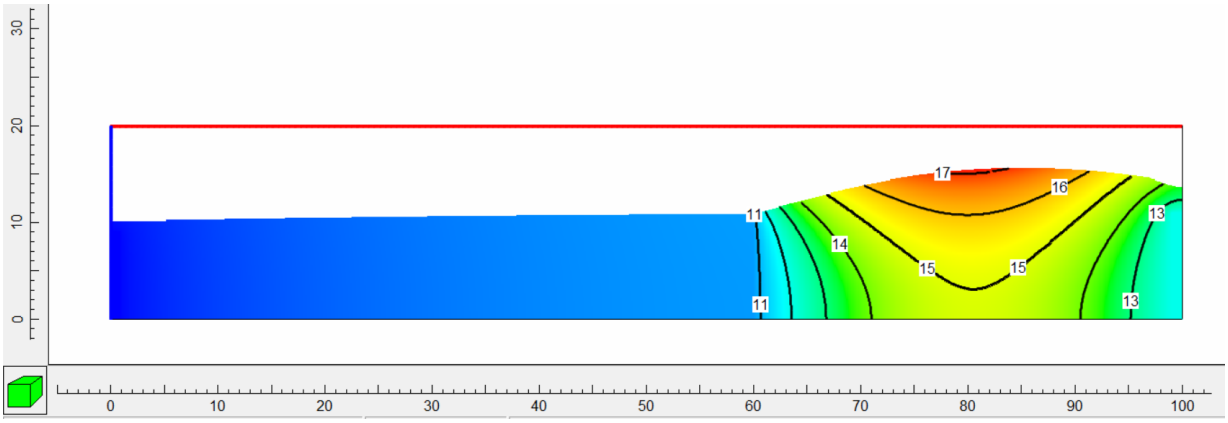

Figure S4: Simulated piezometric head in a grid spacing equal to 10 cm considering initial head equal to 22 m. Colors represent values of piezometric head, black lines show iso-contours and axes indicate distance in the horizontal and vertical directions in meters.

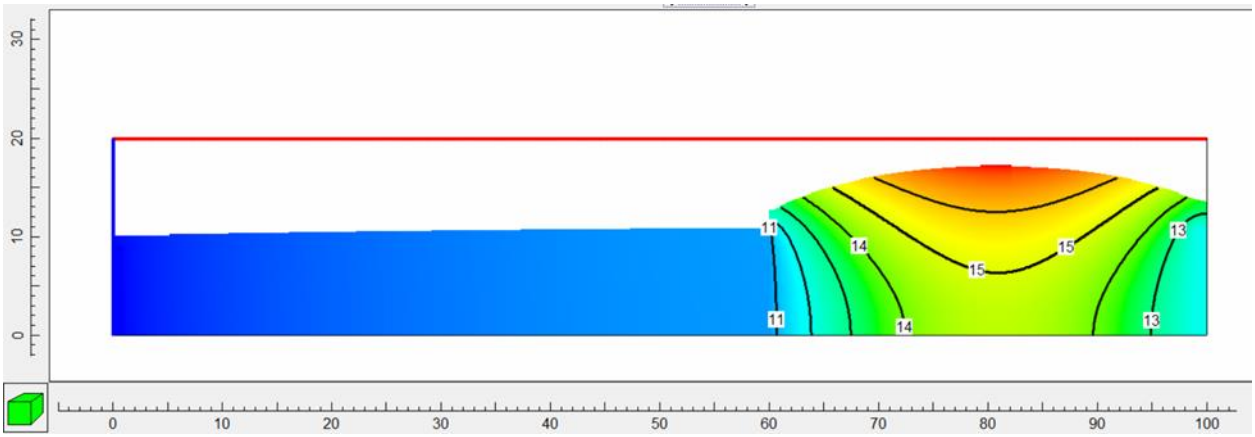

Figure S5: Simulated piezometric head in a grid spacing equal to 10 cm considering initial head equal to 12.5 m. Colors represent values of piezometric head, black lines show iso-contours and axes indicate distance in the horizontal and vertical directions in meters.

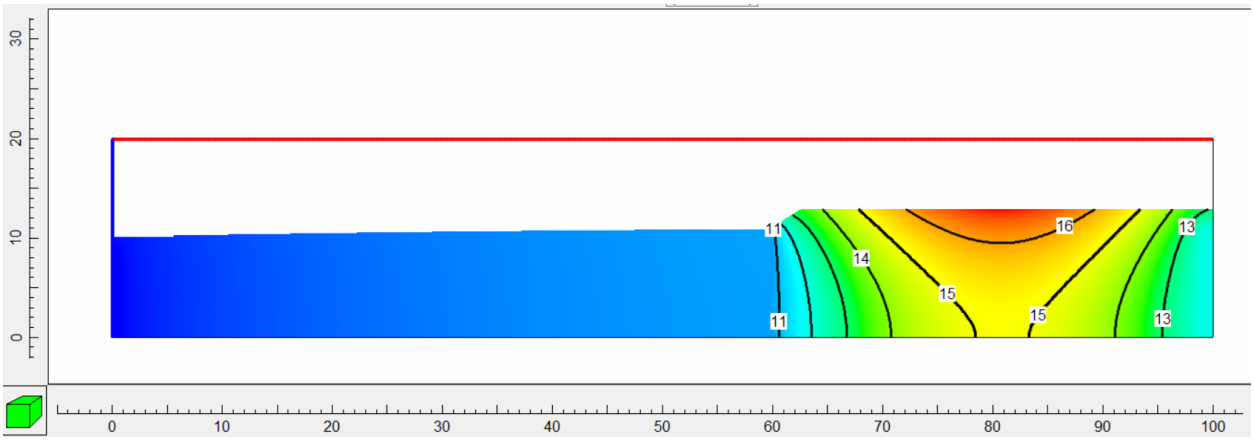

Figure S6: Simulated piezometric head in a grid spacing equal to 10 cm considering initial head equal to 22 m, allowing more external iterations for the non-linear solver. Colors represent values of piezometric head, black lines show iso-contours and axes indicate distance in the horizontal and vertical directions in meters.

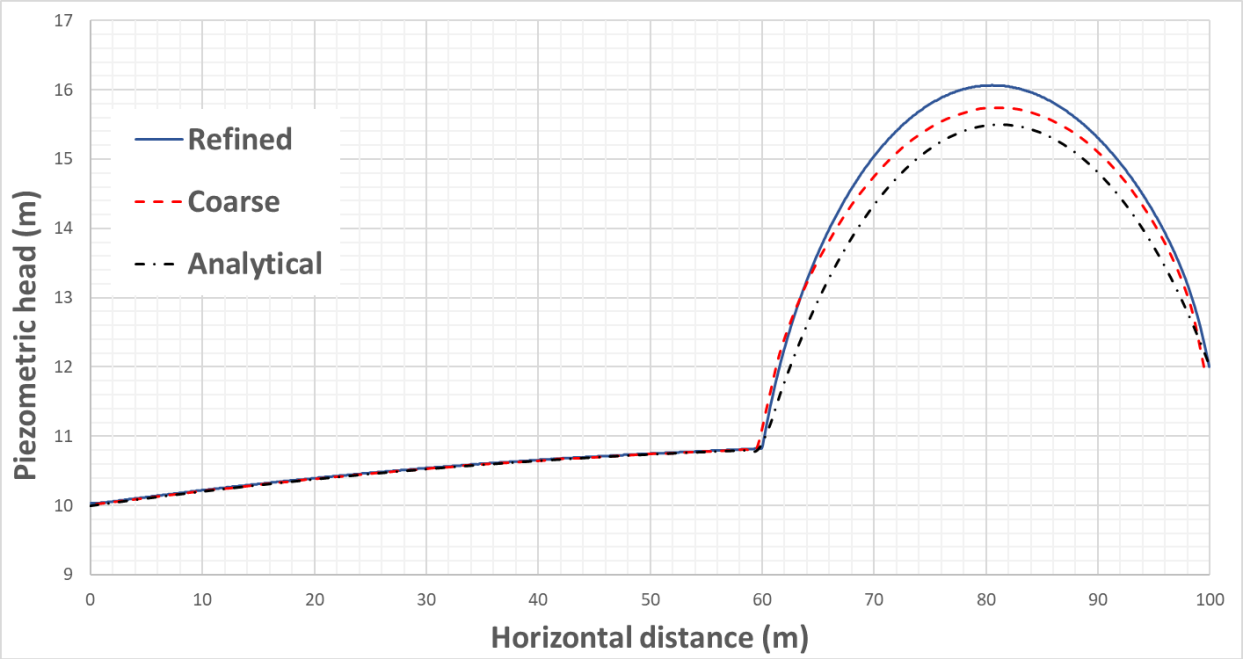

Figure S7: Comparison of analytical and numerical solutions. Numerical solutions correspond to values computed for cells along the row located at the level of the lower boundary condition (z = 10 m).

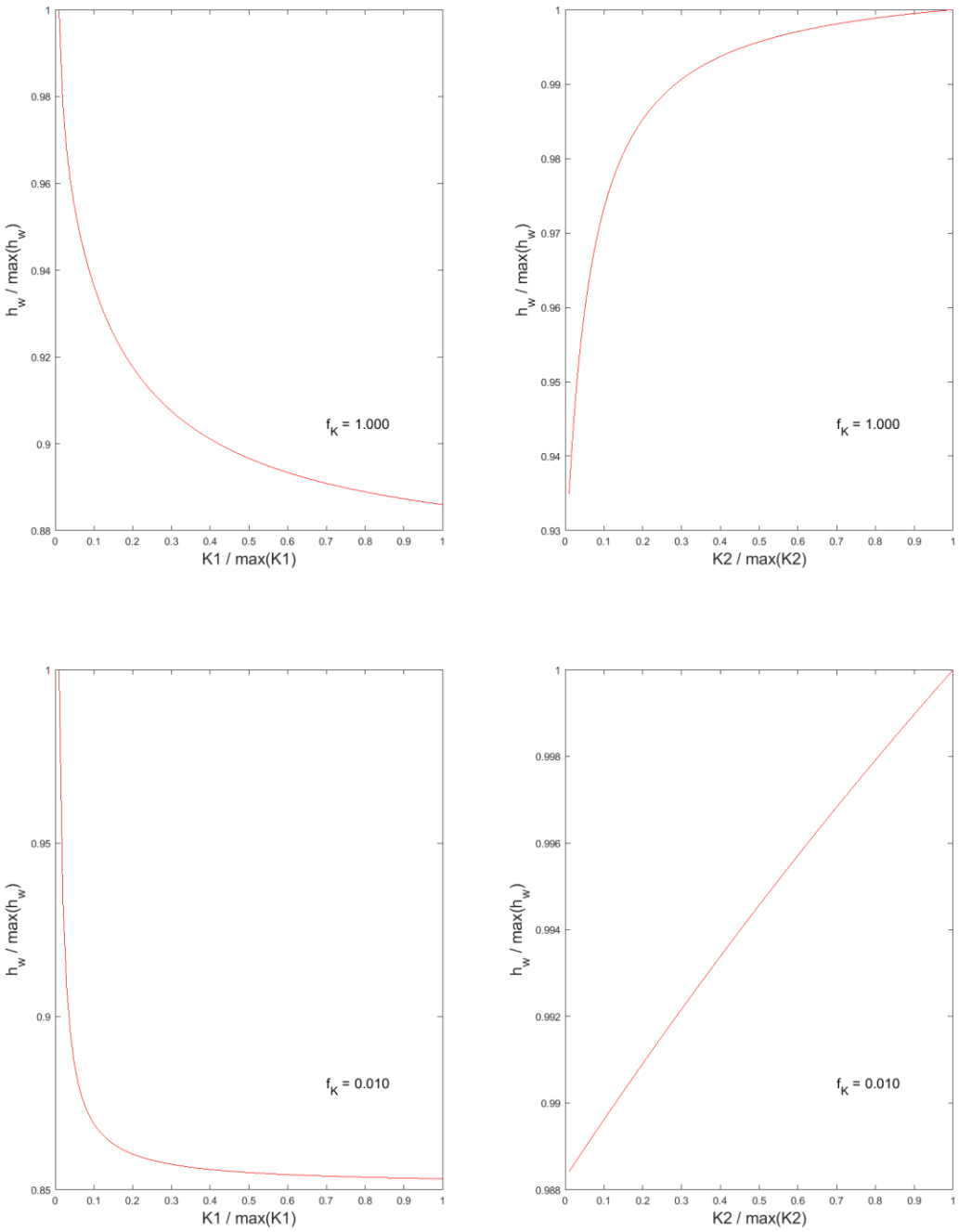

Figure S8: Simulated piezometric level at the well position versus values of hydraulic conductivity in material 1 and 2 (K_1 and K_2). The behavior of the solution can be highly non-linear depending on the ratio between both values of K. To prepare this figure we kept one of the values of K constant and changed only the value of the other parameter.

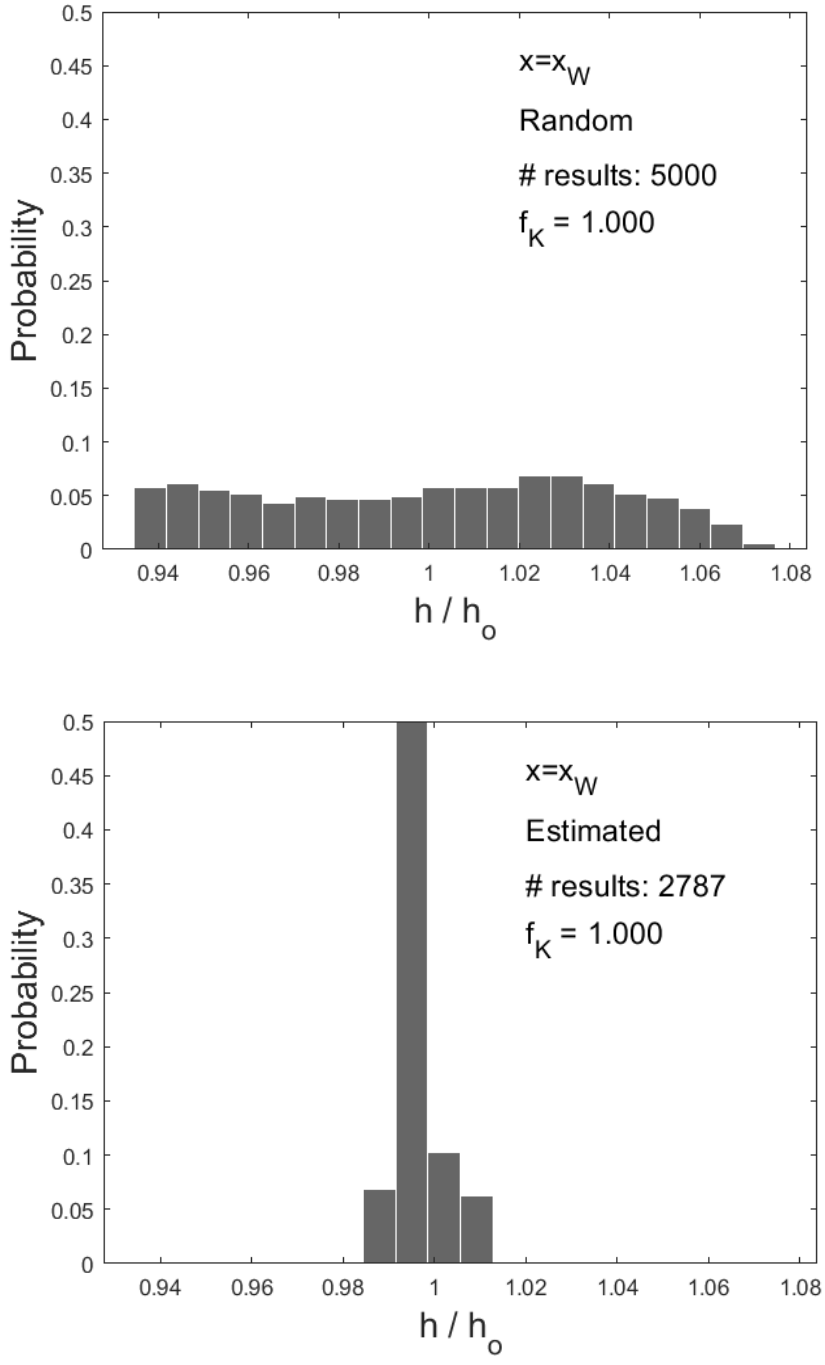

Figure S9: Uncertainy for forecasts of piezometric head at the well position x_w using randomly generated sets of parameters K_1 and K_2 (left) and after parameter estimation (right).

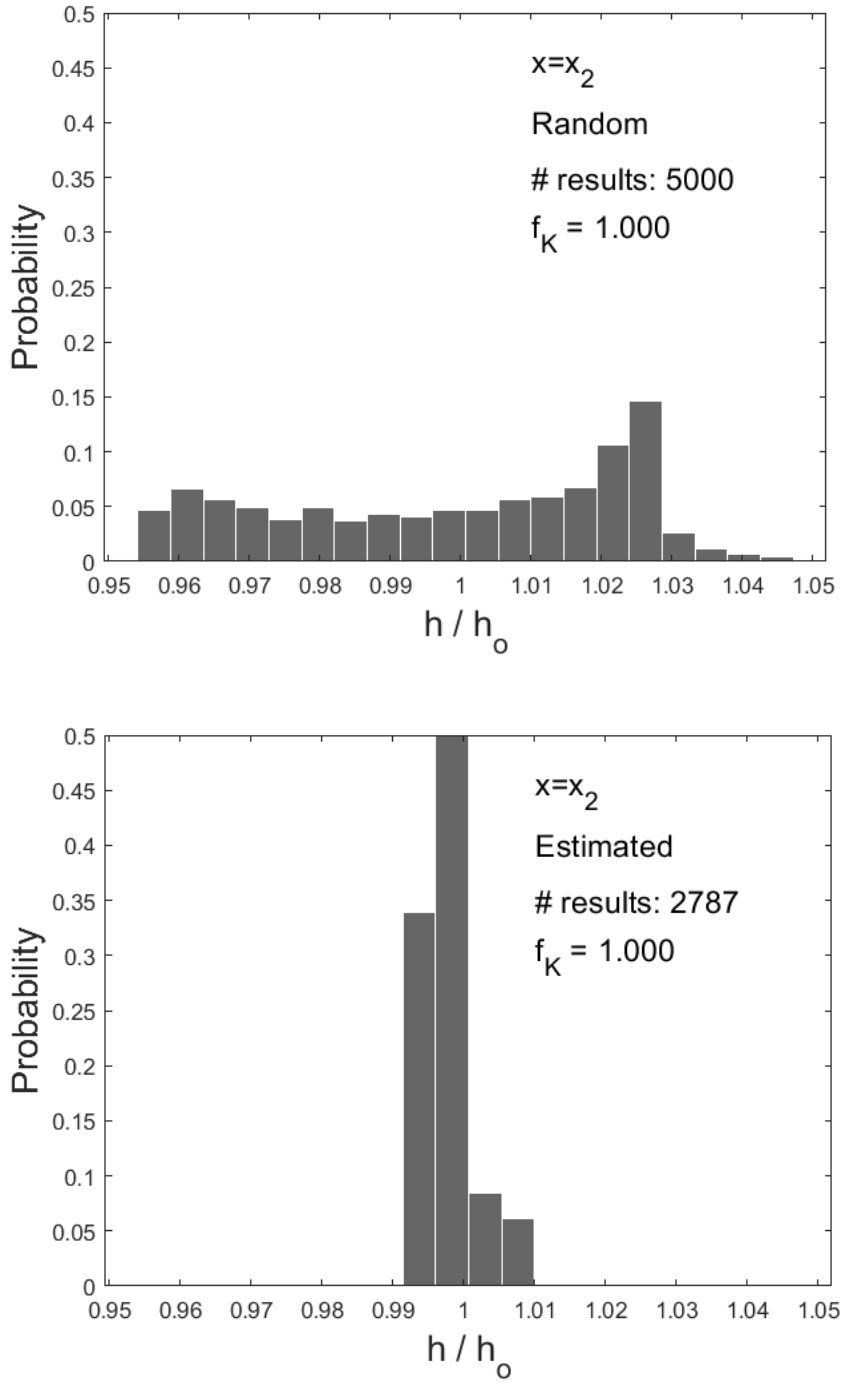

Figure S10: Uncertainy for forecasts of piezometric head at position $x_2 = 0.8\ L$ using randomly generated sets of parameters K_1 and K_2 (left) and after parameter estimation (right).

References:

Harbaugh, A. W. (2005). *MODFLOW-2005, the US Geological Survey modular ground-water model: the ground-water flow process* (pp. 6-A16). Reston, VA: US Department of the Interior, US Geological Survey.

Doherty, J. E., & Hunt, R. J. (2010). *Approaches to highly parameterized inversion: a guide to using PEST for groundwater-model calibration* (Vol. 2010). Reston: US Department of the Interior, US Geological Survey.

Doherty, J. (2015). *Calibration and uncertainty analysis for complex environmental models*. Brisbane, Australia: Watermark Numerical Computing.